

# Aqueous Telluridoindate Chemistry: Water Soluble Salts of Monomeric, Dimeric, and Trimeric In/Te Anions $[\text{InTe}_4]^{5-}$ , $[\text{In}_2\text{Te}_6]^{6-}$ and $[\text{In}_3\text{Te}_{10}]^{11-}$

Johanna Heine and Stefanie Dehnen\*

Fachbereich Chemie and Wissenschaftliches Zentrum für Materialwissenschaften (WZMW), Philipps-  
Universität Marburg, Hans Meerwein Strasse, D-35043 Marburg, Germany, email:  
[dehnen@chemie.uni-marburg.de](mailto:dehnen@chemie.uni-marburg.de)

**SUPPORTING INFORMATION**

## 1. Preliminary investigation of solution behavior by $^{125}\text{Te}$ NMR spectroscopy.

### Methods

$^{125}\text{Te}$  NMR measurements were carried out on saturated solutions in  $\text{D}_2\text{O}$  or ethylenediamine (*en*) using a Bruker DRX 400 MHz spectrometer at 25 °C.  $\text{Me}_2\text{Te}$  was used as internal standard.  $\text{C}_6\text{D}_6$  was used as an external reference in the measurement of the *en* sample.

### Results and discussion

Chalcogenidostannate anions are known to undergo a pH dependent aggregation in solution [1]. However, in high concentration, *i.e.* at high pH value, the anion provided in the solid state is usually the predominant or only one detected upon dissolving the salt. In order to examine, whether our synthetic findings reported herein for the telluridoindate salts are indeed based on a solution behavior different from the stannates, we have recorded  $^{125}\text{Te}$  NMR spectra of as-prepared ' $\text{K}_5\text{InTe}_5$ '.

Solution NMR spectra of telluridoindate anions have not been reported so far. Thus we have measured preliminary  $^{125}\text{Te}$  spectra of a saturated solution of ' $\text{K}_5\text{InTe}_4$ ' in  $\text{D}_2\text{O}$  and in *en*. As depicted in figure S1, two peaks were observed at  $-450$  and  $-993$  ppm, that indicate the presence of an equilibrium upon dissolution of the crude phase in water. The spectrum recorded in *en* shows a single peak at 809 ppm (figure S2). This seems rather peculiar, since  $\text{K}_6[\text{In}_2\text{Te}_6]\cdot 4 \text{ en}$  [2] is the only compound we could obtain from *en* solutions of ' $\text{K}_5\text{InTe}_4$ '. Since there are no available data in literature on In/Se or In/Te NMR spectra, we tried to calculate the NMR signals by quantum chemical methods employing well-established programs. However, owing to the high charge which is mainly accumulated on the Te atoms and possibly the high quadrupole moment of the  $^{115}\text{In}$  nucleus, the results have not been reliable for any of the calculated species, although the charge was compensated for. Thus it is not possible to assign the peaks yet – still, the observation accords well with the crystallization of the salts of diverse telluridoindate anions from the solution of the starting material.

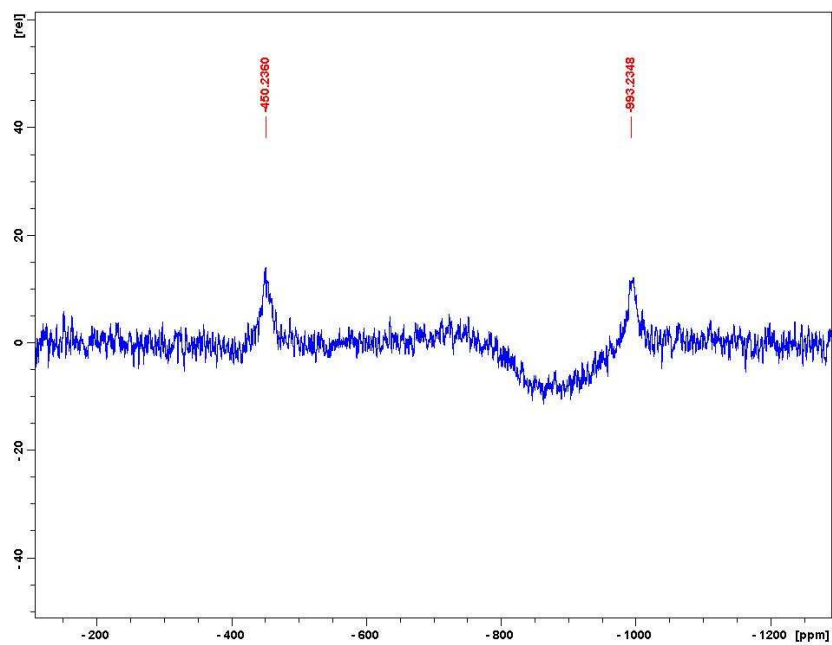


**Figure S1.**  $^{125}\text{Te}$ -NMR spectrum of a saturated solution of as-prepared ' $\text{K}_5\text{InTe}_5$ ' in  $\text{D}_2\text{O}$ .

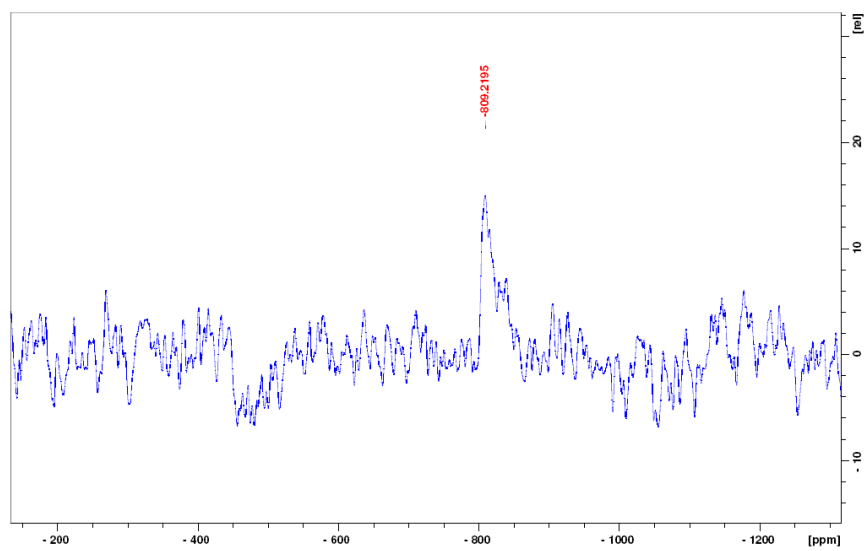


**Figure S2.**  $^{125}\text{Te}$ -NMR spectrum of a saturated solution of as-prepared ' $\text{K}_5\text{InTe}_5$ ' in *en*.

## 2. Raman spectra of telluridoindate salts.

### Methods

Raman spectra were recorded using a Jobin Yvon Labram HR 800 instrument with He/Ne laser excitation ( $\lambda = 632.8$  nm).

### Results and discussion

Raman spectra were recorded on a crystalline sample of known compound  $K_6[In_2Te_6] \cdot 4 en$  [2] (figure S3, top) and a mixture of crystalline compounds  $[K_5(H_2O)_{2.16}][InTe_4]$  (**1**),  $[K_5(H_2O)_5][InTe_4]$  (**2**), and  $[K_6(H_2O)_6][In_2Te_6]$  (**3**) (figure S3, center). Both show a predominant line around  $132\text{ cm}^{-1}$ , along with a broader line of lower intensity between  $150$  and  $180\text{ cm}^{-1}$  for  $K_6[In_2Te_6] \cdot 4 en$ , and several peaks of lower intensity at lower and higher frequencies in the spectrum of the mixture of compounds **1-3**. In order to compare and analyze the spectra, vibrational modes (figure S3, bottom, and tables S1 – S4), were calculated on geometry-optimized anions  $[InTe_4]^{5-}$ ,  $[In_2Te_6]^{6-}$ ,  $[In_3Te_{10}]^{11-}$ , and  $[In_4Te_{10}]^{8-}$  using density functional theory (DFT) [3] methods implemented within the program system TURBOMOLE [4]. The spectrum of  $K_6[In_2Te_6] \cdot 4 en$  is in good accordance with the calculated spectrum of the dimeric anion – disregarding the relative intensity, which is, however, usually not very well reproduced by the calculations. For the mixture of compounds **1-3**, best accordance is achieved for the assumption of a mixture of predominantly  $[InTe_4]^{5-}$  besides lower amounts of  $[In_2Te_6]^{6-}$  and traces of  $[In_3Te_{10}]^{11-}$ , which might have already formed in a low, non-visible concentration. However, it is worth mentioning that (1) the relation of intensities of the Raman modes for different anions are not available through the calculations, (2) the systematic shift of the calculated vibrational modes differs slightly for all species due to different total charges and thus different errors upon charge compensation, and (3) that the vibrational modes at lowest ( $85.8\text{ cm}^{-1}$ ) and highest wavenumbers ( $185.6\text{ cm}^{-1}$ ) can not be assigned to vibrations from the mentioned telluroindate anions. They might, however, arise from impurities upon partial decomposition of the indates.

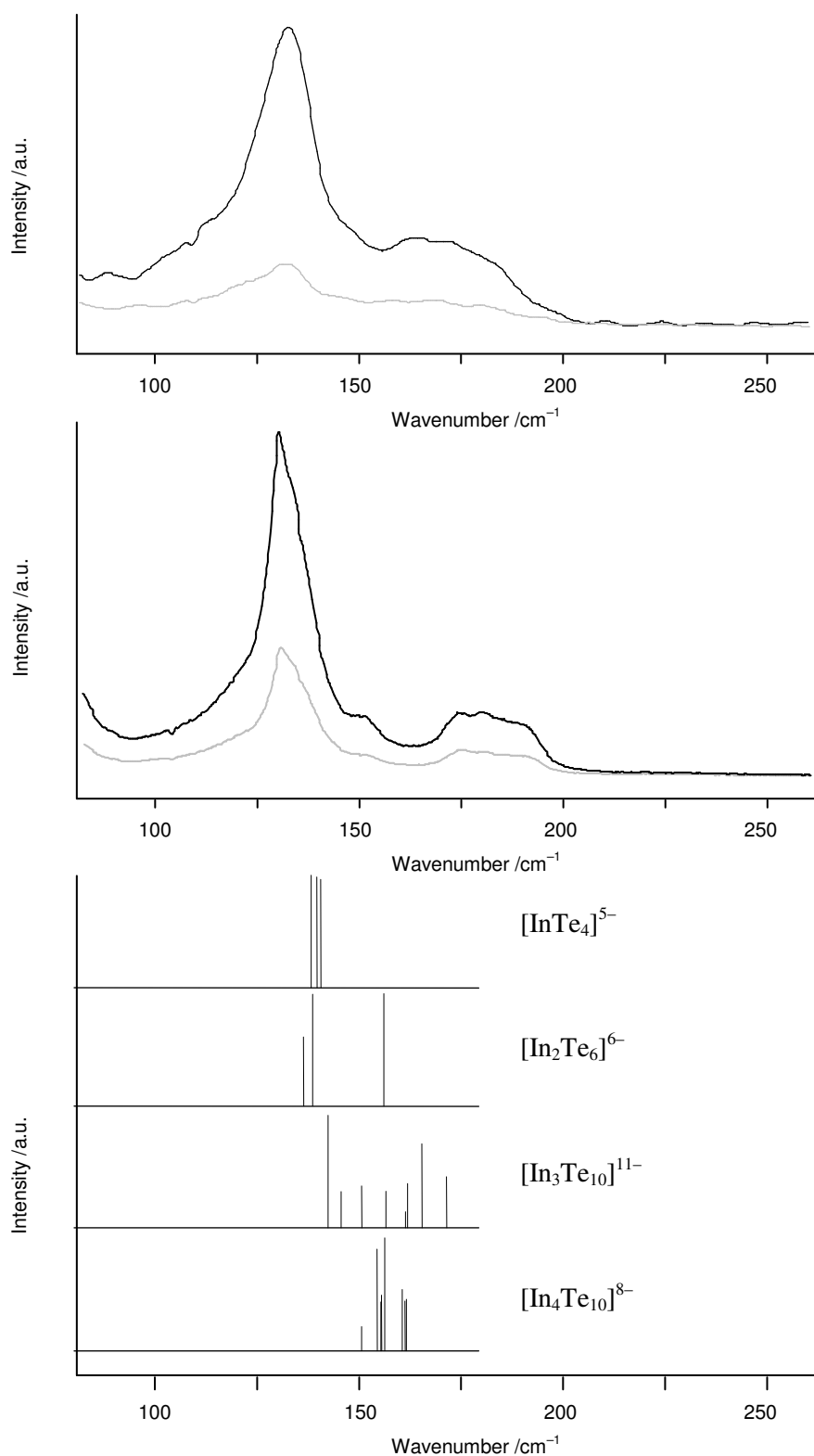


**Figure 9.** Raman spectra of  $K_6[In_2Te_6] \cdot 4 en$  [2] (top) or a mixture of **1-3** (center), with (–) or without (–) polarization filter; comparison with calculated vibrational modes of highest intensities for the DFT structures of  $[InTe_4]^{5-}$ ,  $[In_2Te_6]^{6-}$ ,  $[In_3Te_{10}]^{11-}$ , and  $[In_4Te_{10}]^{8-}$  (bottom).

### 3. Methods of the theoretical investigations

The density functional theoretical (DFT) [3] investigations were undertaken by means of the program system TURBOMOLE [4] using the RIDFT program [5] with the Becke-Perdew (B-P) functional [6] and the gridsize m3. Basis sets were of def2-TZVPP quality (TZVPP = triple zeta valence plus double polarization) [7]. For In and Te atoms effective core potentials (ECP-28) [8] have been used for consideration of relativistic corrections and to reduce the computational effort. The high negative charge was compensated for by employment of the COSMO model [9]. Simultaneous optimizations of geometric and electronic structures were performed without symmetry restrictions, *i.e.* in  $C_1$  symmetry, also allowing for convergence into local minima at higher symmetry. Vibrational spectra were calculated via analytical second derivatives using the program NUMFORCE implemented in TURBOMOLE. For the attempts to calculate  $^{125}\text{Te}$ -NMR shifts, the Te basis set was changed to the all-electron basis TZVPPall without ECP for explicit treatment of inner electrons. The shift values were developed as difference from to the calculated shifts of the experimental standard compound  $\text{TeMe}_2$  which was calculated by the same methods.

**Table S1.** Calculated vibrational spectrum of  $[\text{InTe}_4]^{5-}$  upon simultaneous optimization of geometric and electronic structure of the anion using DFT methods. All modes possess *a* symmetry due to calculation without symmetry restrictions; however, similar frequencies indicate symmetry degenerate modes. Most intense modes are highlighted in red.

<b><math>[\text{InTe}_4]^{5-}</math> * zero point VIBRATIONAL energy : 0.0017482 Hartree *</b>						
mode	1	2	3	4	5	6
frequency	0.00	0.00	0.00	0.00	0.00	0.00
symmetry						
IR	–	–	–	–	–	–
intensity (km/mol)	0.00	0.00	0.00	0.00	0.00	0.00
intensity ( % )	0.00	0.00	0.00	0.00	0.00	0.00
RAMAN	–	–	–	–	–	–
mode	7	8	9	10	11	12
frequency	35.53	38.75	52.93	55.63	58.58	106.36
symmetry	a	a	a	a	a	a
IR	YES	YES	YES	YES	YES	YES
intensity (km/mol)	0.15	0.42	4.56	5.40	2.96	0.27
intensity ( % )	0.09	0.27	2.94	3.49	1.91	0.17
RAMAN	YES	YES	YES	YES	YES	YES
mode	13	14	15			
frequency	<b>138.62</b>	<b>140.02</b>	<b>140.95</b>			
symmetry	a	a	a			
IR	YES	YES	YES			
intensity (km/mol)	155.02	152.72	149.29			
intensity ( % )	<b>100.00</b>	<b>98.52</b>	<b>96.30</b>			
RAMAN	YES	YES	YES			

**Table S2.** Calculated vibrational spectrum of  $[\text{In}_2\text{Te}_6]^{6-}$  upon simultaneous optimization of geometric and electronic structure of the anion using DFT methods. All modes possess *a* symmetry due to calculation without symmetry restrictions; however, similar frequencies indicate symmetry degenerate modes. Most intense modes are highlighted in blue.

<b><math>[\text{In}_2\text{Te}_6]^{6-}</math> * zero point VIBRATIONAL energy : 0.0033501 Hartree *</b>						
mode	1	2	3	4	5	6
frequency	i15.07	0.00	0.00	0.00	0.00	0.00
symmetry	a					
IR	YES	–	–	–	–	–
intensity (km/mol)	0.00	0.00	0.00	0.00	0.00	0.00
intensity ( % )	0.00	0.00	0.00	0.00	0.00	0.00
RAMAN	YES	–	–	–	–	–
mode	7	8	9	10	11	12
frequency	0.00	14.44	28.84	37.19	39.14	40.06
symmetry		a	a	a	a	a
IR	–	YES	YES	YES	YES	YES
intensity (km/mol)	0.00	0.06	0.60	15.58	5.24	15.92
intensity ( % )	0.00	0.02	0.20	5.26	1.77	5.38
RAMAN	–	YES	YES	YES	YES	YES
mode	13	14	15	16	17	18
frequency	42.65	52.31	61.21	71.70	109.22	112.70
symmetry	a	a	a	a	a	a
IR	YES	YES	YES	YES	YES	YES
intensity (km/mol)	5.89	0.21	2.85	1.59	13.17	0.05
intensity ( % )	1.99	0.07	0.96	0.54	4.45	0.02
RAMAN	YES	YES	YES	YES	YES	YES
mode	19	20	21	22	23	24
frequency	113.52	136.71	138.95	155.54	156.57	159.75
symmetry	a	a	a	a	a	a
IR	YES	YES	YES	YES	YES	YES
intensity (km/mol)	0.96	182.18	294.83	2.43	296.04	7.67
intensity ( % )	0.32	61.54	99.59	0.82	100.00	2.59
RAMAN	YES	YES	YES	YES	YES	YES



**Table S3.** Calculated vibrational spectrum of  $[\text{In}_3\text{Te}_{10}]^{11-}$  upon simultaneous optimization of geometric and electronic structure of the anion using DFT methods. All modes possess *a* symmetry due to calculation without symmetry restrictions; however, similar frequencies indicate symmetry degenerate modes. Most intense modes are highlighted in green.

<b><math>[\text{In}_3\text{Te}_{10}]^{11-}</math> * zero point VIBRATIONAL energy : 0.0059950 Hartree *</b>						
mode	1	2	3	4	5	6
frequency	0.00	0.00	0.00	0.00	0.00	0.00
symmetry						
IR	–	–	–	–	–	–
intensity (km/mol)	0.00	0.00	0.00	0.00	0.00	0.00
intensity ( % )	0.00	0.00	0.00	0.00	0.00	0.00
RAMAN	–	–	–	–	–	–
mode	7	8	9	10	11	12
frequency	15.59	17.43	21.53	22.68	24.79	25.78
symmetry	a	a	a	a	a	a
IR	YES	YES	YES	YES	YES	YES
intensity (km/mol)	0.19	1.13	0.43	0.17	0.42	0.91
intensity ( % )	0.08	0.49	0.19	0.07	0.18	0.39
RAMAN	YES	YES	YES	YES	YES	YES
mode	13	14	15	16	17	18
frequency	29.23	34.16	35.70	37.19	40.06	44.99
symmetry	a	a	a	a	a	a
IR	YES	YES	YES	YES	YES	YES
intensity (km/mol)	0.02	0.00	0.16	0.76	0.96	1.27
intensity ( % )	0.01	0.00	0.07	0.33	0.42	0.55
RAMAN	YES	YES	YES	YES	YES	YES
mode	19	20	21	22	23	24
frequency	51.40	54.78	55.38	60.60	61.07	62.49
symmetry	a	a	a	a	a	a
IR	YES	YES	YES	YES	YES	YES
intensity (km/mol)	10.60	1.91	1.58	4.13	29.48	7.28
intensity ( % )	4.59	0.82	0.69	1.78	12.75	3.15
RAMAN	YES	YES	YES	YES	YES	YES
mode	25	26	27	28	29	30
frequency	64.89	68.35	75.40	107.08	108.20	117.41
symmetry	a	a	a	a	a	a
IR	YES	YES	YES	YES	YES	YES
intensity (km/mol)	8.13	0.03	3.90	1.53	0.53	0.80
intensity ( % )	3.52	0.01	1.69	0.66	0.23	0.34
RAMAN	YES	YES	YES	YES	YES	YES
mode	31	32	33	34	35	36
frequency	135.93	142.76	146.01	151.12	157.07	161.92
symmetry	a	a	a	a	a	a
IR	YES	YES	YES	YES	YES	YES
intensity (km/mol)	0.10	231.22	74.05	86.01	74.95	32.73
intensity ( % )	0.05	100.00	32.03	37.20	32.41	14.16
RAMAN	YES	YES	YES	YES	YES	YES
mode	37	38	39			
frequency	162.41	166.01	172.08			
symmetry	a	a	a			
IR	YES	YES	YES			
intensity (km/mol)	90.83	172.59	105.05			
intensity ( % )	39.28	74.64	45.43			
RAMAN	YES	YES	YES			

**Table S4.** Calculated vibrational spectrum of  $[\text{In}_4\text{Te}_{10}]^{8-}$  upon simultaneous optimization of geometric and electronic structure of the anion using DFT methods. All modes possess *a* symmetry due to calculation without symmetry restrictions; however, similar frequencies indicate symmetry degenerate modes. Most intense modes are highlighted in pink.

<b><math>[\text{In}_4\text{Te}_{10}]^{8-}</math> * zero point VIBRATIONAL energy : 0.0074703 Hartree *</b>						
mode	1	2	3	4	5	6
frequency	0.00	0.00	0.00	0.00	0.00	0.00
symmetry						
IR	–	–	–	–	–	–
intensity (km/mol)	0.00	0.00	0.00	0.00	0.00	0.00
intensity ( % )	0.00	0.00	0.00	0.00	0.00	0.00
RAMAN	–	–	–	–	–	–
mode	7	8	9	10	11	12
frequency	29.37	31.51	32.19	32.50	32.75	33.91
symmetry	a	a	a	a	a	a
IR	YES	YES	YES	YES	YES	YES
intensity (km/mol)	1.38	2.08	2.68	2.86	2.47	3.87
intensity ( % )	0.66	1.00	1.28	1.37	1.18	1.85
RAMAN	YES	YES	YES	YES	YES	YES
mode	13	14	15	16	17	18
frequency	35.95	37.05	42.51	44.74	48.06	49.01
symmetry	a	a	a	a	a	a
IR	YES	YES	YES	YES	YES	YES
intensity (km/mol)	7.12	6.84	0.05	0.42	2.69	2.38
intensity ( % )	3.41	3.27	0.02	0.20	1.29	1.14
RAMAN	YES	YES	YES	YES	YES	YES
mode	19	20	21	22	23	24
frequency	49.32	54.45	57.58	58.24	66.45	68.42
symmetry	a	a	a	a	a	a
IR	YES	YES	YES	YES	YES	YES
intensity (km/mol)	3.20	0.27	0.35	0.09	0.63	11.26
intensity ( % )	1.53	0.13	0.17	0.04	0.30	5.39
RAMAN	YES	YES	YES	YES	YES	YES
mode	25	26	27	28	29	30
frequency	69.03	69.75	108.44	113.85	114.25	115.00
symmetry	a	a	a	a	a	a
IR	YES	YES	YES	YES	YES	YES
intensity (km/mol)	13.11	11.62	0.22	11.25	7.04	10.99
intensity ( % )	6.27	5.56	0.10	5.38	3.37	5.26
RAMAN	YES	YES	YES	YES	YES	YES
mode	31	32	33	34	35	36
frequency	150.97	151.76	153.33	154.83	155.55	155.79
symmetry	a	a	a	a	a	a
IR	YES	YES	YES	YES	YES	YES
intensity (km/mol)	45.07	3.67	5.17	188.13	20.03	90.38
intensity ( % )	21.56	1.75	2.47	90.00	9.58	43.24
RAMAN	YES	YES	YES	YES	YES	YES
mode	37	38	39	40	41	42
frequency	155.93	156.72	161.05	161.73	162.06	165.02
symmetry	a	a	a	a	a	a
IR	YES	YES	YES	YES	YES	YES
intensity (km/mol)	102.90	209.03	113.60	92.23	95.70	11.01
intensity ( % )	49.22	100.00	54.34	44.12	45.78	5.27
RAMAN	YES	YES	YES	YES	YES	YES

**Table S5.** Selected bond lengths and angles in compounds **1-6**, as observed in the crystal structures.

Compound	<b>1</b>	<b>2</b>	<b>3</b>	<b>4</b>	<b>5</b>	<b>6</b>
In – Te	2.7660(13)- 2.8566(12)	2.7687(20)- 2.8071(19)	2.7495(9)- 2.8327(14)	2.7064(19)- 2.8597(12)	2.729(4)- 2.870(5)	2.7458(11)- 2.8423(10)
A...Te	3.4217(29)- 3.7971(30)	3.4420(38)- 3.7768(48)	3.4575(14)- 3.8318(15)	3.4270(38)- 3.8782(42)	3.4821(17)- 3.847(7)	3.6116(12)- 3.9427(15)
A...O	2.6052(389)- 3.3135(314)	2.6257(142)- 2.9143(184)	2.7076(32)- 2.7682(31)	2.6614(187)- 3.0675(135)	2.7419(247)- 3.4597(86)	2.8776(86)- 3.4120(63)
Te...(H)O	3.4393(90)- 3.5895(99)	3.4951(162)- 3.7080(201)	3.4719(31)- 3.6539(34)	3.4387(228)- 3.8438(351)	3.5627(232)- 3.8539(223)	3.5275(64)- 3.8997(69)
In-In <sup>a</sup>	6.9307(3)- 7.9027(4)	7.4045(9)- 7.7899(10)	8.9926(18)- 10.7786(17)	7.6394(8)- 11.4831(12)	11.0105(7)	8.8811(18)- 10.5438(23)
Te-In-Te	103.27(4)- 113.02(4)	107.84(6)- 111.12(6)	110.429(15)- 114.72(3)	103.29(6)- 113.448(18)	92.1(2) -113.6(2)	108.87(3)- 115.63(3)
Coordination motifs of A	K...O <sub>3</sub> Te <sub>3</sub> , K...O <sub>2</sub> Te <sub>5</sub> , K...O <sub>2</sub> Te <sub>4</sub> , K...O <sub>1</sub> Te <sub>5</sub> , K...O <sub>1</sub> Te <sub>4</sub> , K...Te <sub>5</sub>	K...O <sub>4</sub> Te <sub>2</sub> , K...O <sub>3</sub> Te <sub>2</sub> , K...O <sub>2</sub> Te <sub>4</sub> , K...Te <sub>5</sub>	K...O <sub>2</sub> Te <sub>4</sub>	K...O <sub>3</sub> Te <sub>2</sub> , K...O <sub>2</sub> Te <sub>4</sub> , K...Te <sub>6</sub>	K...O <sub>1</sub> Te <sub>5</sub> , K...O <sub>2</sub> Te <sub>6</sub> , K...Te <sub>3</sub> , K...Te <sub>5</sub> , K...Te <sub>6</sub>	Rb...O <sub>4</sub> Te <sub>4</sub> , Rb...O <sub>3</sub> Te <sub>4</sub> , Rb...O <sub>2</sub> Te <sub>5</sub>
Coordination motifs of Te	Te...InK <sub>6</sub> , Te...InK <sub>6</sub> O <sub>1</sub> , Te...InK <sub>3</sub> O <sub>3</sub> , Te...InK <sub>5</sub> O <sub>1</sub> , Te...InK <sub>6</sub> O <sub>2</sub> , Te...InK <sub>3</sub> O <sub>3</sub>	Te...InK <sub>5</sub> , Te...InK <sub>5</sub> O <sub>1</sub> , Te...InK <sub>4</sub> O <sub>1</sub>	Te...In <sub>2</sub> K <sub>4</sub> O <sub>2</sub> , Te...InK <sub>5</sub> O <sub>1</sub> , Te...InK <sub>3</sub> O <sub>2</sub>	Te...In <sub>2</sub> K <sub>5</sub> , Te...InK <sub>7</sub> , Te...InK <sub>6</sub> , Te...InK <sub>5</sub> O <sub>1</sub> , Te...InK <sub>3</sub> O <sub>4</sub>	Te...In <sub>2</sub> K <sub>3</sub> , Te...InK <sub>7</sub> , Te...InK <sub>6</sub> , Te...InK <sub>5</sub>	Te...In <sub>2</sub> Rb <sub>3</sub> O <sub>1</sub> , Te...InRb <sub>4</sub> O <sub>3</sub> , Te...InRb <sub>6</sub> O <sub>3</sub>

<sup>a</sup> Distance of the barycenters of the dimeric and trimeric anions in compounds **3-6**.

## References

- [1] Krebs, B. *Angew. Chem. Int. Ed.* **1983**, 22, 113-134.
- [2] Wang, C.; Haushalter, R. C. *Inorg. Chem.* **1997**, 36, 3806-3807.
- [3] a) Parr, R. G.; Yang, W. *Density Functional Theory of Atoms and Molecules*, Oxford University Press, New York **1988**; b) Ziegler, T. *Chem. Rev.* **1991**, 91, 651–667.
- [4] a) Ahlrichs, R.; Bär, M.; Häser, M.; Horn, H.; Kölmel, C. *Chem. Phys. Lett.* **1989**, 162, 165; b) Treutler, O.; Ahlrichs, R. *J. Chem. Phys.*, **1995**, 102, 346–354.
- [5] a) Eichkorn, K.; Treutler, O.; Öhm, H.; Häser, M.; Ahlrichs, R. *Chem. Phys. Lett.* **1995**, 242, 652–660; b) Eichkorn, K.; Weigend, F.; Treutler, O.; Ahlrichs, R. *Theor. Chim. Acta* **1997**, 97, 119–124.
- [6] a) Becke, A.D. *Phys. Rev. A* **1988**, 38, 3098-3109; b) Vosko, S.H.; Wilk, L.; Nusair, M. *Can. J. Phys.* **1980**, 58, 1200–1205; c) Perdew, J.P. *Phys. Rev. B* **1986**, 33, 8822–8837.
- [7] Weigend, F.; Ahlrichs, R. *Phys. Chem. Chem. Phys.* **2005**, 7, 3297-3305.
- [8] a) Metz, B.; Stoll, H.; Dolg, M. *J. Chem. Phys.* **2000**, 113, 2563-2569; b) Te: Peterson, K.A.; Figgen, D.; Goll, E.; Stoll, H.; Dolg, M.; *J. Chem. Phys.* **2003**, 119, 11113-11123.
- [9] a) Klamt, A.; Schürmann, G. *J. Chem. Soc. Perkin Trans.* **1993**, 5, 799–805; b) Schäfer, A.; Klamt, A.; Sattel, D.; Lohrenz, J.C.W.; Eckert, F. *Phys. Chem. Chem. Phys.* **2000**, 2, 2187- 2193.